

Northumbria Research Link

Citation: Sfikas, Athanasios, Gonzalez Sanchez, Sergio, Lekatou, Angeliki G., Kamnis, Spyros and Karantzalis, Alexandros E. (2022) A Critical Review on Al-Co Alloys: Fabrication Routes, Microstructural Evolution and Properties. *Metals*, 12 (7). p. 1092. ISSN 2075-4701

Published by: MDPI

URL: <https://doi.org/10.3390/met12071092> <<https://doi.org/10.3390/met12071092>>

This version was downloaded from Northumbria Research Link:
<http://nrl.northumbria.ac.uk/id/eprint/49405/>

Northumbria University has developed Northumbria Research Link (NRL) to enable users to access the University's research output. Copyright © and moral rights for items on NRL are retained by the individual author(s) and/or other copyright owners. Single copies of full items can be reproduced, displayed or performed, and given to third parties in any format or medium for personal research or study, educational, or not-for-profit purposes without prior permission or charge, provided the authors, title and full bibliographic details are given, as well as a hyperlink and/or URL to the original metadata page. The content must not be changed in any way. Full items must not be sold commercially in any format or medium without formal permission of the copyright holder. The full policy is available online: <http://nrl.northumbria.ac.uk/policies.html>

This document may differ from the final, published version of the research and has been made available online in accordance with publisher policies. To read and/or cite from the published version of the research, please visit the publisher's website (a subscription may be required.)





**Northumbria
University**
NEWCASTLE



UniversityLibrary

Review

A Critical Review on Al-Co Alloys: Fabrication Routes, Microstructural Evolution and Properties

Athanasios K. Sfikas ^{1,*}, Sergio Gonzalez ¹, Angeliki G. Lekatou ², Spyros Kamnis ³
and Alexandros E. Karantzalis ²

¹ Faculty of Engineering and Environment, Northumbria University, Newcastle upon Tyne NE1 8ST, UK; sergio.sanchez@northumbria.ac.uk

² Department of Materials Science and Engineering, University of Ioannina, 45110 Ioannina, Greece; alekatou@uoi.gr (A.G.L.); akarantz@uoi.gr (A.E.K.)

³ Castolin Eutectic-Monitor Coatings Ltd., Newcastle upon Tyne NE29 8SE, UK; spyros.kamnis@castolin.com

* Correspondence: athanasios.sfikas@northumbria.ac.uk or thanasfi@gmail.com

Abstract: Al-Co alloys is an emerging category of metallic materials with promising properties and potential application in various demanding environments. Over the years, different manufacturing techniques have been employed to fabricate Al-Co alloys, spanning from conventional casting to rapid solidification techniques, such as melt spinning, thus leading to a variety of different microstructural features. The effect of the fabrication method on the microstructure is crucial, affecting the morphology and volume of the precipitates, the formation of supersaturated solid solutions and the development of amorphous phases. In addition, the alloy composition has an effect on the type and volume fraction of intermetallic phases formed. As a result, alloy properties are largely affected by the microstructural outcomes. This review focuses on highlighting the effect of the fabrication techniques and composition on the microstructure and properties of Al-Co alloys. Another goal is to highlight areas in the field that are not well understood. The advantages and limitations of this less common category of Al alloys are being discussed with the scope of future prospects and potential applications.

Keywords: Al-Co alloys; vacuum arc melting; stir casting; melt spinning; rapid solidification; Al₉Co₂; Al₁₃Co₄; Al₅Co₂; Al corrosion; Al wear



Citation: Sfikas, A.K.; Gonzalez, S.; Lekatou, A.G.; Kamnis, S.; Karantzalis, A.E. A Critical Review on Al-Co Alloys: Fabrication Routes, Microstructural Evolution and Properties. *Metals* **2022**, *12*, 1092. <https://doi.org/10.3390/met12071092>

Academic Editors: Elvira Oñorbe and Judit Medina

Received: 21 May 2022

Accepted: 21 June 2022

Published: 26 June 2022

Publisher's Note: MDPI stays neutral with regard to jurisdictional claims in published maps and institutional affiliations.



Copyright: © 2022 by the authors. Licensee MDPI, Basel, Switzerland. This article is an open access article distributed under the terms and conditions of the Creative Commons Attribution (CC BY) license (<https://creativecommons.org/licenses/by/4.0/>).

1. Introduction

Aluminium and its alloys are of interest due to their light weight, high specific strength and high stiffness. Among them, those containing transition metals have attracted a lot of attention over the last years including Al-Cr [1,2], Al-V [3–5], Al-Ti [6] and Al-Ni [7–10] alloys due to their hardness and corrosion resistance. Moreover, combining transition metal additions with non-equilibrium fabrication conditions enables to significantly enhance the hardness and corrosion resistance, leading to improved properties compared to commercial Al alloys [11].

Amongst all the transition metals, cobalt is a less common addition to Al alloys. It has been reported that minor Co additions can increase the microstructural stability of Al-Fe-Si intermetallics [12] and modify their geometry from long rod-like shape to Chinese script [13]. Small Co additions can also be used to alter the microstructure of Al-Ni alloys, promoting the refinement of Al₃Ni fibers [14]. One of the first references on binary Al-Co alloys was back in 1926 when Samuel Daniels manufactured various compositions and assessed their microstructure and their mechanical and corrosion properties [15]. Renewed interest in Al-Co alloys surfaced in the last few decades mainly due to the development of rapid solidification fabrication processes [16–18], the discovery of quasicrystals/complex metallic alloys [19–22], and the observation of metadislocations (metadislocations are highly complex structural defects involving hundreds of atoms) [23].

Another field of high interest for Al-Co alloys that attracted a lot of attention is the surface, catalytic and transport properties of Al-Co intermetallic compounds [24–33]. During the last decade, the focus shifted on the fabrication of bulk Al-Co alloys, using non-equilibrium techniques such as vacuum arc melting, and the assessment of their surface degradation properties. The effect of the fabrication method and composition on the microstructure and properties has been the focus of several works [34,35]. In another recent work, the use of Al-Co intermetallics as ex situ reinforcement in Al-based composites has been studied, highlighting the versatility of the material [36]. More recently, Al-Co alloys have been successfully fabricated with modern fabrication techniques such as additive manufacturing, exhibiting good mechanical properties [37].

To the best of the authors' knowledge, this is the first effort to compile and study the literature on Al-Co alloys, which is an uncommon family of Al alloys. The focus of this critical review is to discuss different aspects of Al-Co alloys produced using non-equilibrium and conventional processing techniques. In addition, phase constitution, manufacturing techniques, microstructures, mechanical, corrosion and wear behavior will be discussed. The main goal of this work is to discuss the effect of the fabrication method and composition on the microstructural outcome and final properties of Al-Co alloys. In more detail, the focus is to compare different fabrication routes involving a variety of solidification rates and study the effect of the cooling rate on the microstructure and final properties of Al-Co alloys. Additionally, a wide range of Co compositions have been studied, spanning from 0.5 wt % to 47.2 wt % Co, i.e., from microalloying to main alloying element concentrations. To provide a systematic study, different Al-Co alloys have been assessed, from low Co-containing alloys exhibiting high ductility to Al-Co alloys with a higher Co content and therefore a large volume fraction of intermetallics. Furthermore, it is attempted to highlight areas that have not been sufficiently studied and are not well understood. A tentative outlook commenting the challenges, future prospects and potential applications of Al-Co alloys is also presented.

2. Al-Co Phase Constitution

From the Al-Co equilibrium phase diagram, several equilibrium phases can be identified including Al solid solution, α -Co solid solution, cph ϵ -Co solid solution, monoclinic Al_9Co_2 , c-centered monoclinic $\text{Al}_{13}\text{Co}_4$, Al_3Co , hexagonal Al_5Co_2 and AlCo with CsCl structure. A eutectic reaction takes place at 1.1 wt % Co ($l \rightarrow \text{Al} + \text{Al}_9\text{Co}_2$) with an eutectic temperature of 657 °C. The maximum solubility of Co in Al is negligible at room temperature (Figure 1a) [38]. Other studies reported that the maximum solubility of Co in Al is 0.04 wt % Co [39]. While the stability and the structure of Al_9Co_2 and Al_5Co_2 are well established, many different thermodynamically stable phases in between have been identified (Table 1). These include the quasicrystalline approximant τ^2 - $\text{Al}_{13}\text{Co}_4$ [19], orthorhombic O- $\text{Al}_{13}\text{Co}_4$, monoclinic M- $\text{Al}_{13}\text{Co}_4$, Y-phase and Z-phase [40,41]. The Z-phase corresponds to the intermetallic Al_3Co and has been associated with τ^2 - $\text{Al}_{13}\text{Co}_4$ [40]. Other phases that have been identified in the vicinity of $\text{Al}_{13}\text{Co}_4$ include a new approximant O'- $\text{Al}_{13}\text{Co}_4$ crystallizing in the orthorhombic system [42] (O'- $\text{Al}_{13}\text{Co}_4$ is considered a high temperature modification of O- $\text{Al}_{13}\text{Co}_4$ [43]), a stable monoclinic Y_1 - $\text{Al}_{13}\text{Co}_4$ and the metastable orthorhombic Y_2 - $\text{Al}_{13}\text{Co}_4$ [43]. Several recent efforts have been focused on revisiting the Al-Co phase diagram (Figure 1b) [43–45].

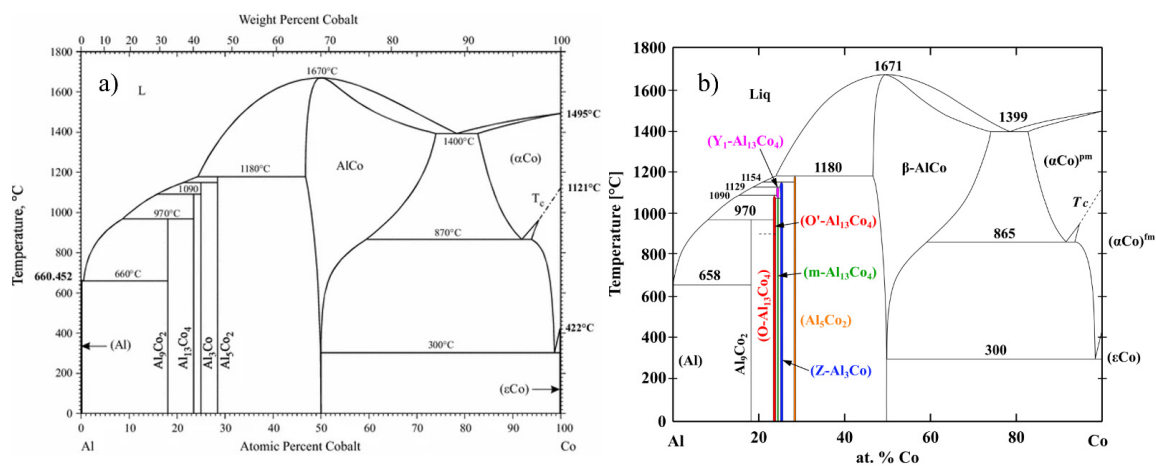


Figure 1. (a) Al-Co equilibrium phase diagram [46,47] (Reprinted with permission from [46]. Copyright 2022, Springer Nature), (b) Revisited Al-Co equilibrium phase diagram [43,45,48].

Table 1. Crystallographic data for the intermetallic compounds present in the Al-Co system.

Phase	Space Groups	a (Å)	b (Å)	c (Å)	β (°)	References
Al ₉ Co ₂	P2 ₁ /C	6.21	6.28	8.55	94.77	[49,50]
Y ₁ -Al ₁₃ Co ₄	C2/m (12)	17.06	4.10	7.50	116.02	[43]
Y ₂ -Al ₁₃ Co ₄	Immm (71)	12.03	7.58	15.35	-	[43]
O-Al ₁₃ Co ₄	Pmn2 ₁	8.15	12.34	14.45	-	[41,51,52]
O'-Al ₁₃ Co ₄	Pnma	28.89	8.13	12.34	-	[42]
M-Al ₁₃ Co ₄	C2/m	15.17	8.10	12.34	107.84	[53,54]
Z-Al ₃ Co	P2/m	39.83	8.12	32.18	108.03	[55–60]
Al ₅ Co ₂	P6 ₃ /mmc	7.67	-	7.60	-	[61–63]
B2-AlCo	Pm-3m	2.86	-	-	-	[64,65]

3. Microstructural Analysis

3.1. The Effect of the Fabrication Route on the Microstructure

High cooling rates (i.e., rapid solidification) promote the microstructural refinement and extension of the solid solution. For certain metallic alloys with high glass-forming ability, they can be obtained in an amorphous state upon rapid cooling. For one Al-Co composition, the microstructure can be easily tuned through control of the cooling rate, as will be shown in this section.

Over the years, Al-Co alloys have been successfully fabricated using various non-equilibrium techniques including wedge-shaped copper mold casting [66], melt spinning [67], gun quenching [17], laser glazing [68], directional solidification casting [69], vacuum arc melting [70] and additive manufacturing [37]. These fabrication methods involve different cooling rates, for example 10^5 – 10^7 K/s for melt spinning [17], 10^8 – 10^{10} K/s for gun quenching [17] and 10–100 K/s for vacuum arc melting [71]. Other works focused on the employment of near equilibrium conventional techniques and solid-state diffusion-based techniques including stir casting and powder metallurgy [34,72].

Optimization of the composition, the cooling rate and their combined effect enables achieving an endless spectrum of microstructures and therefore of mechanical performances. For this reason, it is of great importance from the scientific point of view and engineering application to select the best combination of composition and cooling rate. Here, below, we provide insight about a few of these combinations reported in the literature. For example, the effect of the cooling rate on the microstructure has been studied in detail in an Al-2.6 wt % Co alloy that has been solidified with different cooling rates. A slow cooling rate (2 K/s) leads to the formation of a microstructure with primary Al₉Co₂ crystals and eutectic Al/Al₉Co₂ lamellar phase of acicular morphology. However, when

the solidification rate is faster (10^4 K/s), a quasi-eutectic microstructure consisting of an Al solid solution and Al_9Co_2 is observed, and therefore, the preferential growth of primary phases is suppressed [73]. This is consistent with what could be expected, since rapid solidification promotes the formation of supersaturated solid solution. This means the elements prefer to remain in solid solution rather than segregate toward grain boundaries or existing phases and therefore can lead to more refined microstructures. Rapid solidification also enables microstructures to depart from equilibrium eutectic. The microstructure can be further refined, and the homogeneity improved with the employment of melt superheating (heating the melt in temperature much higher than the melting point) and increased cooling rates (10^6 K/s). The supersaturated Al solid solution is in an unstable state, and therefore, annealing results in closer to equilibrium microstructures. For example, annealing at 350 °C leads to the decomposition and segregation of fine secondary Al_9Co_2 phase of 10 nm average size [74].

As commented, the solubility of Co in Al is very low, and therefore, in order to retain more Co in solid solution (i.e., supersaturation), one has to rapidly cool the alloy. This leads to a supersaturated Al solid solution with an extended area of solid solution. For example, several different values of maximum solubility of Co in Al have been reported including 1.1 wt % Co [74], 1.1–10.3 wt % Co [75], 1.1–2.2 wt % Co [68], 5 wt % Co [17], 3.6 wt % Co [18], and 5.5 wt % Co [76], which are several orders of magnitude above the maximum solubility of Co in Al under equilibrium conditions [38,39]. It is important to take into consideration that in several techniques such as melt spinning or vacuum arc melting, the cooling rate is not homogenous across the fabricated sample. For example, in melt spinning, the surface of the ribbon in direct contact with the fast-cooling copper wheel results in a faster cooling rate than the opposite surface of the ribbon in contact with the air. Likewise, in vacuum arc melting, the surface of the sample in direct contact with the water-cooled copper hearth solidifies faster than the center of the sample. In addition, smaller samples cool down faster than larger samples, thus resulting in finer microstructures and higher concentrations of Co dissolved in Al. Melt spun Al-Co alloys of different compositions (5.3–19.5 wt % Co) may exhibit a variety of microstructural features including coarse primary Al_9Co_2 , fine Al_9Co_2 or primary Al dendrites with Co segregated interdendrically. There is a strong dependence of these features on the local cooling rate [16]. These findings were validated by another work on a hypereutectic Al-Co alloy (Al-5 wt % Co), indicating that depending on the cooling rate, a variety of microstructural outcomes can be observed including a supersaturated solid solution or primary Al_9Co_2 developed within the Al matrix [17]. Features including a supersaturated solid solution, fine dendrites, coarse dendrites and a mixture of slightly supersaturated solid solution and massive Al_9Co_2 particles have been observed with a decreasing cooling rate in melt spun Al-Co alloys (5.1–42 wt % Co). Another interesting observation is the formation of an amorphous phase at very high cooling rates. The critical cooling rate for the formation of the amorphous phase in the Al-Co system is $>10^8$ K/s [18]. Nonetheless, due to the rapid solidification employed in melt spinning, the supersaturated Al solid solution may become unstable, leading to decomposition with annealing. After annealing, the formation of monoclinic Al_9Co_2 precipitates in a Widmanstätten pattern, and a close orientation relation with the matrix has been reported in an Al-5 wt % Co alloy [77].

Depending on the fabrication technique, different cooling rates are achieved, which ultimately has an effect on the microstructure of the alloys. For example, for an Al-7 wt % Co alloy fabricated by stir casting, vacuum arc melting and powder metallurgy, a variety of microstructures have been reported including coarse blades of primary Al_9Co_2 randomly dispersed in the Al matrix along with fine platelets of lamellar Al_9Co_2 for the stir cast alloy (Figure 2), and large elongated eutectic “colonies” consisting of strips of Al_9Co_2 within Al for the vacuum arc melted alloy (Figure 2). On the other hand, Al-7 wt % Co fabricated by powder metallurgy exhibited a microstructure with coarse rounded agglomerates of Al_9Co_2 dispersed within the Al matrix (Figure 2). For all fabrication methods, the microstructures consisted of Al_9Co_2 precipitates uniformly distributed in the Al matrix.

This can be attributed to the fact that the composition falls within the Al-Al₉Co₂ area of the equilibrium phase diagram. Nonetheless, the vacuum arc melted alloy exhibited the highest hardness values due to the largest volume fraction of the hard Al₉Co₂ intermetallic phase, the high quantities of Co dissolved in the Al matrix and the greatest fraction of Al-Al₉Co₂ boundaries [34]. The question that arises is whether the processing route will have exactly the same effect on the microstructure for the different compositions of the Al-Co alloy system. To answer this question, microstructural differences for the Al-32 wt % Co alloy fabricated by stir casting, vacuum arc melting and powder metallurgy have been compared. Diverse phases in different volume fractions were reported in each case. The stir cast and arc-melted alloy (Figure 2) had similar microstructures consisting of mostly a primary Al₁₃Co₄ phase surrounded by Al₉Co₂ and a small volume fraction of aluminum at the interphase. However, the volume fraction of Al₉Co₂ in the vacuum arc melted alloy was reduced compared to the stir cast counterpart, which was due to the rapid solidification rate that prohibited the completion of the peritectic reaction that leads to the formation of Al₉Co₂. The microstructure of the powder metallurgy processed Al-32 wt % Co alloy consisted of a variety of intermetallic compounds, including Al₉Co₂, Al₁₃Co₄, and Al₅Co₂ within the Al matrix (Figure 2). The presence of multiple phases has been correlated with the preparation method that is governed by solid-state diffusion mechanisms. As a result, layers corresponding to different phases have been formed [72].

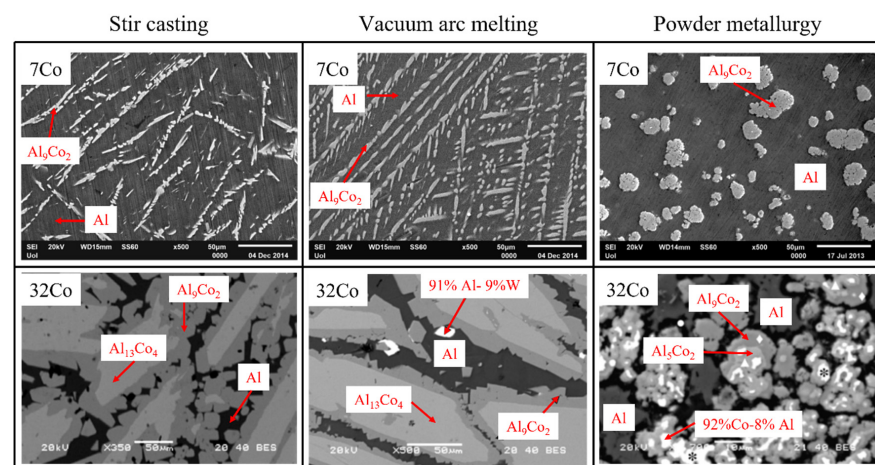


Figure 2. SEM images (backscattered electron mode) for Al-7 wt % Co (7Co) and Al-32 wt % Co (32Co) fabricated by stir casting, vacuum arc melting and powder metallurgy (Reprinted with permission from [34,72]. Copyright 2022, Elsevier).

3.2. The Effect of the Composition on the Microstructure

The composition can have a great influence on the microstructure since, as shown in Figure 1, the nature and volume fraction of the phases formed varies with the composition. For certain processing routes, the nature and volume fraction of the precipitates formed will vary with the concentration of cobalt. In this section, the different microstructures for the Al-Co system will be discussed in terms of concentration of cobalt.

For example, for relatively small concentrations of cobalt, from 0 up to about 32wt % Co, i.e., in the Al-Al₉Co₂ part of the Al-Co phase diagram, a variety of microstructures have been reported. This compositional area is the most important from the engineering point of view since there is interest in developing alloys as light and as strong as possible, which is a compromise that can only be achieved with small cobalt additions. For Al-Co alloys fabricated by water-cooled mold casting, in Al-1.5 wt % Co, the eutectic microstructure prevails and additionally, depending on the cooling rate, eutectic colonies with either small fractions of Al or Al₉Co₂ phase are formed. For 0.7–1 wt % Co, a eutectic mixture of α -Al-Al₉Co₂ coexists with the Al matrix. Microstructural differences result in different mechanical properties such as in the hardness. For example, the hypereutectic composition (Al-1.5 wt % Co) is approximately 41% harder than the eutectic (Al-1 wt % Co) and the

hypoeutectic (Al-0.7 wt % Co) Al-Co alloys. This has been attributed to the increasing volume fraction of the hard Al_9Co_2 intermetallic phase with increasing Co content [69]. The hardness of Al-Co alloys increases with increasing Co content, which is attributed to the increase in the volume fraction of Al_9Co_2 and increasing Co dissolved within the Al matrix [35,76]. Several works focused on Al-Co alloys with different cobalt additions, from 2 wt % Co up to 20 wt % Co, in the hypereutectic region using vacuum arc melting [76,78]. Despite the hypereutectic compositions, for Al-Co alloys containing up to 10 wt % Co, eutectic morphology prevails (Figure 3). This has been attributed to the non-equilibrium microstructures produced due to the fast-cooling rate. However, increasing Co content leads to increasing primary morphological features. For example, Al-15 wt % Co shows a mixed morphology with primary Al_9Co_2 and eutectic Al_9Co_2 -Al (Figure 3). Regarding Al-20 wt % Co (Figure 3), the primary morphology dominates [76,78]. The main features that have been reported in this vast range of Co contents (2–20 wt % Co) include eutectic morphology for the lower compositions, directional growth, brick-like mode of growth and side branching. For 2–5 wt % Co, a dual fibrous eutectic microconstituent with a lamellar eutectic microconstituent has been reported [35]. Similar microstructural outcomes have been reported in vacuum arc melted Al-Co alloys (1.1–6.3 wt % Co). In an Al-1.1 wt % Co alloy, pro-eutectic Al prevails. As the Co content increases, there is a transition from eutectic microconstituents (2.2 wt % Co) to coarse dendrites of Al_9Co_2 surrounded by Al with pockets of eutectics in between (6.3 wt % Co) [70].

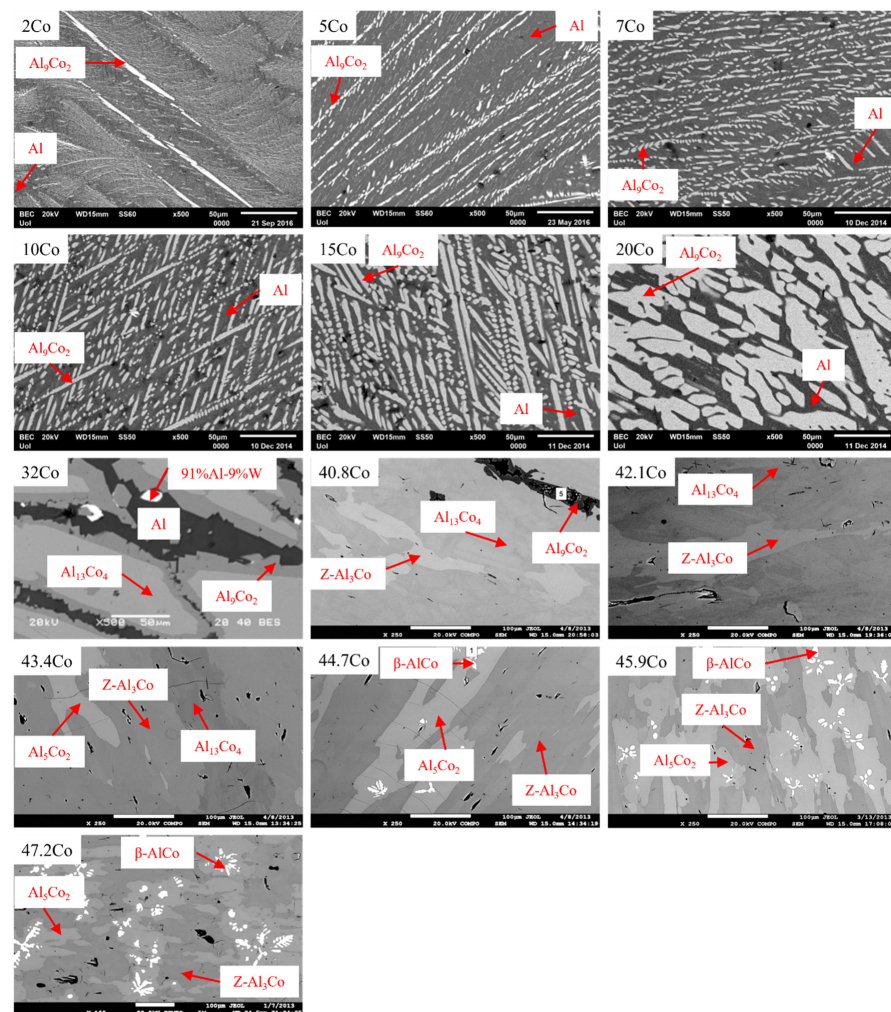


Figure 3. Microstructures (SEM, backscattered electron mode) for Al-Co alloys with different Co compositions (wt % Co) fabricated by vacuum arc melting [72,78–80] (Reprinted with permission from ref. [72,79,80]. Copyright 2022, Elsevier).

Other works focused on studying Al-Co alloys with higher Co content (>32 wt % Co), with concentrations from Al-40.8 wt % Co up to Al-47.2 wt % Co fabricated by vacuum arc melting (Figure 3). According to the results, Al-40.8 wt % Co consists of Z-Al₃Co, Al₁₃Co₄, and Al₉Co₂. On the other hand, Al-42.1 wt % Co and Al-43.4 wt % Co comprise Al₅Co₂, Z-Al₃Co, Al₁₃Co₄, Al-44.7 wt % Co phase constitution includes Al₅Co₂, Z-Al₃Co, while Al-45.9 wt % Co and Al-47 wt % Co consists of β -AlCo, Al₅Co₂ and Z-Al₃Co [79,80]. The presence of multiple different phases in each composition indicates that the fast-cooling rates inhibit the completion of the reactions that lead to the formation of the equilibrium phases. This is consistent with the fact that after annealing Al-43.4 wt % Co and Al-47.2 wt % Co alloys, the phase formation reactions are completed successfully, leading to the formation of an equilibrium microstructure. For example, after annealing at 1050 °C for 330 h, Al-43.4 wt % Co consists of Al₅Co₂, Z-Al₃Co while for Al-47.2 wt % Co, the phases β -AlCo and Al₅Co₂ are present [81].

4. Mechanical Properties and Deformation Mechanisms

As commented previously, small additions of Co can have a dramatic effect on the mechanical performance of Al, and therefore, it is of great scientific and technological importance to comment on the scarce existing literature about the mechanical properties of the Al-Co alloy system. Previous reports focused on the mechanical properties of a single intermetallic phase. For example, the mechanical properties and deformation mechanisms of the intermetallic Al₁₃Co₄ has been studied by several authors [82–84]. However, few works have studied the mechanical properties of the binary Al-Co system. For example, Daniels studied the mechanical properties of sand-cast Al-Co alloys (0.5–10 wt % Co). According to the results, the ultimate strength increases for additions up to 1 wt % Co. However, for Co additions beyond 2 wt %, the ultimate tensile strength decreases below that of the monolithic Al. Likewise, a minor Co addition of 0.5 wt % Co appears to improve the ductility, but further additions decrease the ductility [15]. In situ micropillar compression tests on Al-Co films deposited on Si by magnetron sputtering revealed that when Al-11.9 wt % Co alloy is in a supersaturated solid solution state, it exhibits high flow stresses with significant strain-hardening ability. This behavior was attributed to the presence of incoherent twin boundaries in Al-Co alloys, which may act as a strong barrier for dislocation motion under uniaxial compression tests. A most interesting observation is that ultra-strong Al-Co alloys may have strength comparable to high-strength steels [85]. In another recent work, the effect of modest Co additions in the mechanical properties of additive manufactured Al was studied. According to the findings, 0.5 wt % Co may enhance the tensile properties of the material (Figure 4). This was attributed to the cumulative effect of solid solution strengthening and precipitation hardening. Another effect of Co addition was the elimination of large pores, therefore leading to tensile properties similar to that of medium-strength Al alloys. However, greater Co additions led to an increase in defects and to embrittlement [37]. Taking the above into consideration, it is concluded that in order to improve the understanding of the mechanical properties and deformation mechanisms of Al-Co alloys, more research is needed. In more detail, it is important to understand how different fabrication techniques affect the mechanical properties, especially comparing fabrication techniques with different solidification rates. Another field of great interest is to understand the effect of Co content on the mechanical properties of Al-Co alloys. Correlation of the microstructural features such as the shape and the density of precipitates, the formation of supersaturated solid solutions and the formation of other phases on the mechanical properties of the system would improve the understanding of the deformation behavior of the system.

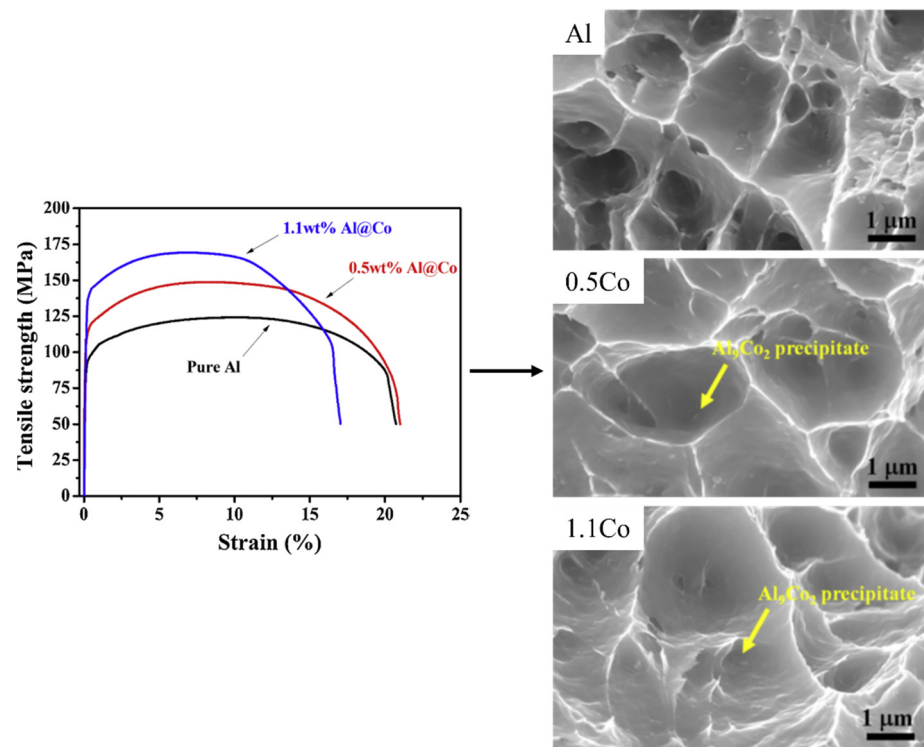


Figure 4. Tensile testing curves for Al, Al-0.5 wt % Co and Al-1.1 wt % Co fabricated by additive manufacturing and associated images of the fractured surface of tensile bars under SEM (Reprinted with permission from [37], Copyright 2022, Elsevier).

5. Corrosion Behavior

5.1. The Effect of the Fabrication Route on the Corrosion Behavior

The good corrosion resistance of Al-Co alloys makes them desirable for applications in demanding environments. However, the corrosion performance not only depends on the composition but also on the microstructure, which in turn varies with the processing route. Two competing mechanisms will determine if the corrosion resistance increases or decreases. A high cooling rate promotes the dissolution of an alloying element, therefore preventing precipitation and the resultant formation of galvanic pairs. However, if the concentration of alloying element is very high and the cooling rate is not enough to keep them in solid solution, they will precipitate and promote the formation of galvanic pairs and therefore promote corrosion. Taking this into consideration, the effect of the cooling rate on the corrosion behavior will be explored in this section for relatively low and high concentrations of cobalt, 7 wt % and 32 wt %.

For example, the corrosion behavior of Al-7 wt % Co alloy fabricated by stir casting, vacuum arc melting and powder metallurgy was assessed in 3.5% NaCl solution by Lekatou et al. [34] (3.5% NaCl solution is a solution of artificial sea water [86]). The authors observed that Al-7 wt % Co alloys exhibited high resistance to localized forms of corrosion in 3.5% NaCl solution, regardless of the manufacturing method. The localized corrosion was associated with the pitting of Al that evolved to crevicing. Nonetheless, Al_3Co_2 remained free of corrosion. Amongst the different configurations, the alloy that was fabricated by vacuum arc melting exhibited the best corrosion performance due to the lower porosity and the dissolution of Co in the Al matrix, thus leading to a less intense galvanic effect between the matrix and the intermetallic compound. Another factor that enhanced the corrosion performance of the vacuum arc melted Al-7 wt % Co alloy was the dense and uniform intermetallic network that constitutes a more effective barrier to the electrolyte penetration through the dissolved Al compared to the stir cast and powder metallurgy processed counterparts [34]. The improved corrosion performance

of the vacuum arc melted alloy over the other configurations was attributed to the more refined microstructure due to the fast-cooling rate employed during the fabrication [34]. The effect of the fabrication method on the corrosion behavior of Al-Co alloys has been highlighted in an Al-32 wt % Co alloy fabricated by stir casting, vacuum arc melting and powder metallurgy. Regardless of the preparation method, the studied alloys exhibited low susceptibility to localized forms of corrosion in 3.5% NaCl solution. The vacuum arc melted alloy exhibited the best corrosion performance due to the highest volume fraction of $\text{Al}_{13}\text{Co}_4$ and the low porosity. Localized corrosion for the vacuum arc melted and the stir cast alloys has been associated with the pitting of the Al matrix. Nonetheless, Al_9Co_2 demonstrated very good corrosion performance, while $\text{Al}_{13}\text{Co}_4$ remained free of corrosion, which was possibly due to lack of electrical contact with the Al matrix and the absence of a galvanic effect with Al_9Co_2 [72]. It is worth mentioning that both Al-7 wt % Co and Al-32 wt % Co, regardless of the manufacturing method, exhibited considerably improved resistance to localized forms of corrosion in 3.5% NaCl compared to the monolithic Al and Al alloys (Al1050, Al6061) [34,72]. Al has very good corrosion resistance due to the formation of a very thin surface oxide film (passive film) [87]. However, the integrity of the passive film is compromised in the presence of aggressive anions such as halides in acidic and alkaline pH conditions [88]. The corrosion resistance of Al may be further decreased with the addition of alloying elements. The electrochemical characteristics of the secondary phases may be very different compared to the Al matrix; therefore, a micro-galvanic cell is formed, leading to localized corrosion [87–89].

5.2. The Effect of the Composition on the Corrosion Behavior

The alloy composition has a critical role in the microstructure (see Section 3.2) and therefore on the corrosion behavior. It is well known that pure aluminum has high corrosion resistance and that the addition of an alloying element in small concentrations would promote the formation of galvanic pairs and thus result in a decrease in the corrosion resistance.

For example, the effect of the Co content on the corrosion behavior of Al-Co alloys (7–20 wt % Co) in 3.5% NaCl has been the focus of a recent work [76]. According to the results, the Co concentration does not appear to have a significant effect on the corrosion behavior of vacuum arc melted Al-Co alloys in the Al- Al_9Co_2 system (7–20 wt % Co) in 3.5% NaCl. It was thus concluded that all compositions exhibit good resistance to localized forms of corrosion in 3.5% NaCl. On the other hand, Al-7 wt % Co had slightly higher corrosion performance compared to the other compositions (10–20 wt % Co). This has been attributed to the formation of a relatively uniform surface film [76]. In Al-Co alloys with higher Co contents (40.8–47.2 wt % Co), anodic dissolution has been identified as the main corrosion mechanism in 3.5% NaCl solution [79,80]. For the lower Co containing compositions (40.8–45.9 wt % Co), pitting corrosion due to chloride anions has been observed. It was deduced that the relative concentration of the phases and the physical contact between them are important for the corrosion behavior of the system [80]. This has been attributed to the increased nobility of Al-Co intermetallics with increasing Co content [79,80].

The importance of the electrolyte type on the corrosion behavior of Al-Co alloys was demonstrated in an Al-43.4 wt % Co alloy annealed at 1050 °C for 330 h. In both NaCl (3.5% NaCl) and HCl (0.01 M) environments, pitting corrosion was observed, while in NaOH (0.01 M), uniform corrosion occurred (Figure 5). Nonetheless, NaOH was the most aggressive corrosion environment, while HCl was the least aggressive for this alloy [81].

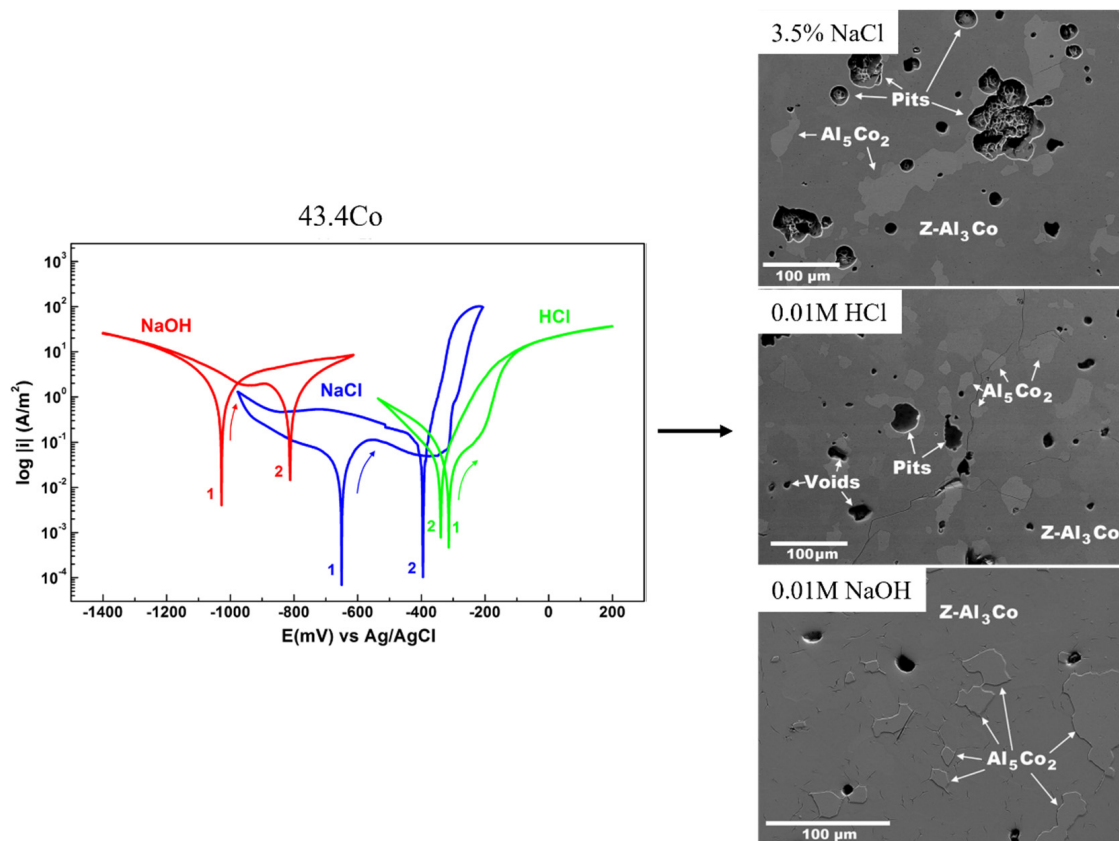


Figure 5. Potentiodynamic polarization curves for Al-43.4 wt % Co in 3.5% NaCl, 0.01M HCl, 0.01M NaOH and corroded surfaces under SEM after polarization (Reprinted with permission from [81], Copyright 2022, Springer Nature).

The importance of the electrolyte on the corrosion performance of Al-Co alloys was further investigated in a recent work on vacuum arc melted Al-Co alloys (2–20 wt % Co) in 1M H₂SO₄ [78]. It is worth mentioning that sulfuric acid is an important chemical used in various industries such as mineral processing, oil refining and wastewater processing. It is thus critical to assess the corrosion performance of a new alloy in this environment with the scope of potential application in various demanding industries. Al-Co alloys exhibited high resistance to localized forms of corrosion in 1M H₂SO₄, especially for the higher compositions (≥ 7 wt % Co). On the other hand, Co addition in Al did not decrease the rate of uniform corrosion. Nonetheless, the studied Al-Co compositions had greater passivation ability than monolithic Al, Al7075-T6, Al2024-T3. It is worth mentioning that the passivation behavior of the lower Co containing Al-Co alloys (2–5 wt % Co) in 1M H₂SO₄ was correlated with the passivation of the Al matrix. On the other hand, for the higher compositions (≥ 7 wt % Co), the passivation behavior was governed initially by the passivation of the Al matrix and at a second stage by the passivation of Al₉Co₂ [80]. High-temperature oxidation of Al-Co alloys (40.8 and 47.2 wt % Co) in a flowing synthetic air environment led to the selective oxidation and the formation of a protective alumina scale on the alloy surfaces. Oxidation kinetics followed a parabolic law rate. The high Al content in both compositions contributed to the good oxidation performance, as the continuous Al₂O₃ scale that was formed acted as a barrier to Co diffusion, and it hindered the nucleation and growth of Co oxides [48].

6. Wear Performance

6.1. The Effect of the Fabrication Route on the Wear Performance

Aluminum, as with other lightweight metals, tends to exhibit poor wear resistance and low hardness, which limits its application in industry. This can be overcome through control of the composition (i.e., alloying) and the processing conditions to promote different wear resistant microstructures. Since Co has very low solubility in aluminum, small additions of cobalt are enough to promote the formation of hard wear-resistant intermetallic phases. For example, Al-7 wt % Co alloy fabricated by stir casting and vacuum arc melting exhibited considerably low wear rates under sliding wear (AISI 52100 steel counter body) compared to monolithic Al [34]. This behavior has been attributed to the strengthening effect of hard Al_9Co_2 intermetallics in the soft matrix that may postpone/inhibit plastic deformation phenomena by reducing the load transfer to the matrix and decreasing the direct contact between area between the matrix and the counterbody [90–92]. Furthermore, Al_9Co_2 provides thermal stability to the matrix, and it provides support to the oxide layer [90–92]. Another interesting finding is that Al-7 wt % Co fabricated by vacuum arc melting and stir casting exhibited improved wear performance over Al1050, Al6060, Al7075-T6, and A356. The vacuum arc melted alloy had better wear behavior compared to the stir cast alloy due to the higher volume fraction of Al_9Co_2 and finer and denser network of intermetallic compounds, highlighting the beneficial effect of the microstructural refinement due to non-equilibrium processing in the wear behavior of Al-Co alloys [34].

6.2. The Effect of the Composition on the Wear Performance

The effect of Al_9Co_2 in the sliding wear performance (AISI 52100 steel counter body) of Al-Co alloys in a wide range of compositions (2–20 wt % Co) has been the focus of a recent work (Figure 6) [35]. According to the results, the wear rate of Al-Co alloys decreases with increasing Co content due to increasing volume fraction of Al_9Co_2 intermetallics from 19 vol % (Al-2 wt %Co) to 63 vol % (Al-20 wt % Co). This can be clearly discerned from the study of the wear tracks (Figure 6), indicating that as the Co content increases, the width of the wear tracks decreases. The beneficial action of Al_9Co_2 in strengthening the Al matrix can be attributed to another factor: the matrix–particle bond. In this case, the Al_9Co_2 intermetallic is formed in situ, and therefore, the Al- Al_9Co_2 interface bond is strong, which is beneficial to achieve high wear resistance [35]. Increasing additions of Co results in a higher volume fraction of Al_9Co_2 and therefore in a reduction in the Al matrix surface area, thus leading to a reduction in possible paths for plastic deformation [90–92]. While the reinforcing action of Al_9Co_2 is well established, the formation of an Al supersaturated solid solution due to the fast cooling rate achieved during fabrication with vacuum arc melting is another potential strengthening factor, which can be attributed to the fact that the dislocation movement is obstructed by the severely deformed supersaturated lattice [35]. It is worth noticing that even a modest addition of 2 wt % Co led to a lower wear rate than several commercial Al alloys (Al1050, Al6060, A356, Al7075), while the compositions rich in Co (≥ 10 wt % Co) demonstrated improved wear resistance over age-treated Al-7Mg-5Si, which is much harder and wear resistant than the other studied commercial Al alloys (Figure 6) [35]. From the point of view of engineering design, it is important to understand the wear mechanisms responsible for the differences in the wear behavior with increasing Co addition. When the concentration of cobalt is small (2–7 wt % Co), the wear processes are dominated by plastic deformation of the Al matrix. However, as the concentration of Co increases to 10 wt % Co, the volume fraction of Al matrix is reduced, and the dominant wear mechanism is sliding abrasive action by plastic deformation. For 15–20 wt % Co, the volume fraction of the Al matrix is further reduced, and as a result, abrasion is the main wear mechanism [35]. However, not always adding more Co, and therefore promoting the formation of Al_9Co_2 , is beneficial to enhance the wear resistance. Since Al_9Co_2 is a brittle phase, increasing the volume fraction of this intermetallic will decrease the ductility of the Al alloy. While the reinforcing action of Al_9Co_2 in Al-Co alloys during sliding wear is well established, a drawback of the increasing volume fraction of Al_9Co_2 is the decreasing

ductility. This effect has been highlighted in hypereutectic Al-Co alloys (7–20 wt % Co) in solid particle erosion tests with the use of angular Al_2O_3 particles as the erodent medium. According to the results, the studied Al-Co alloys demonstrated lower wear resistance than Al at 60° and 90° impact angles, which was attributed to the increasing brittleness of the alloys with increasing Co content. The main degradation mechanisms for Al-Co alloys during solid particle erosion were plastic flow constraint, crack propagation and intersection, causing fracture and the removal of Al_9Co_2 [93].

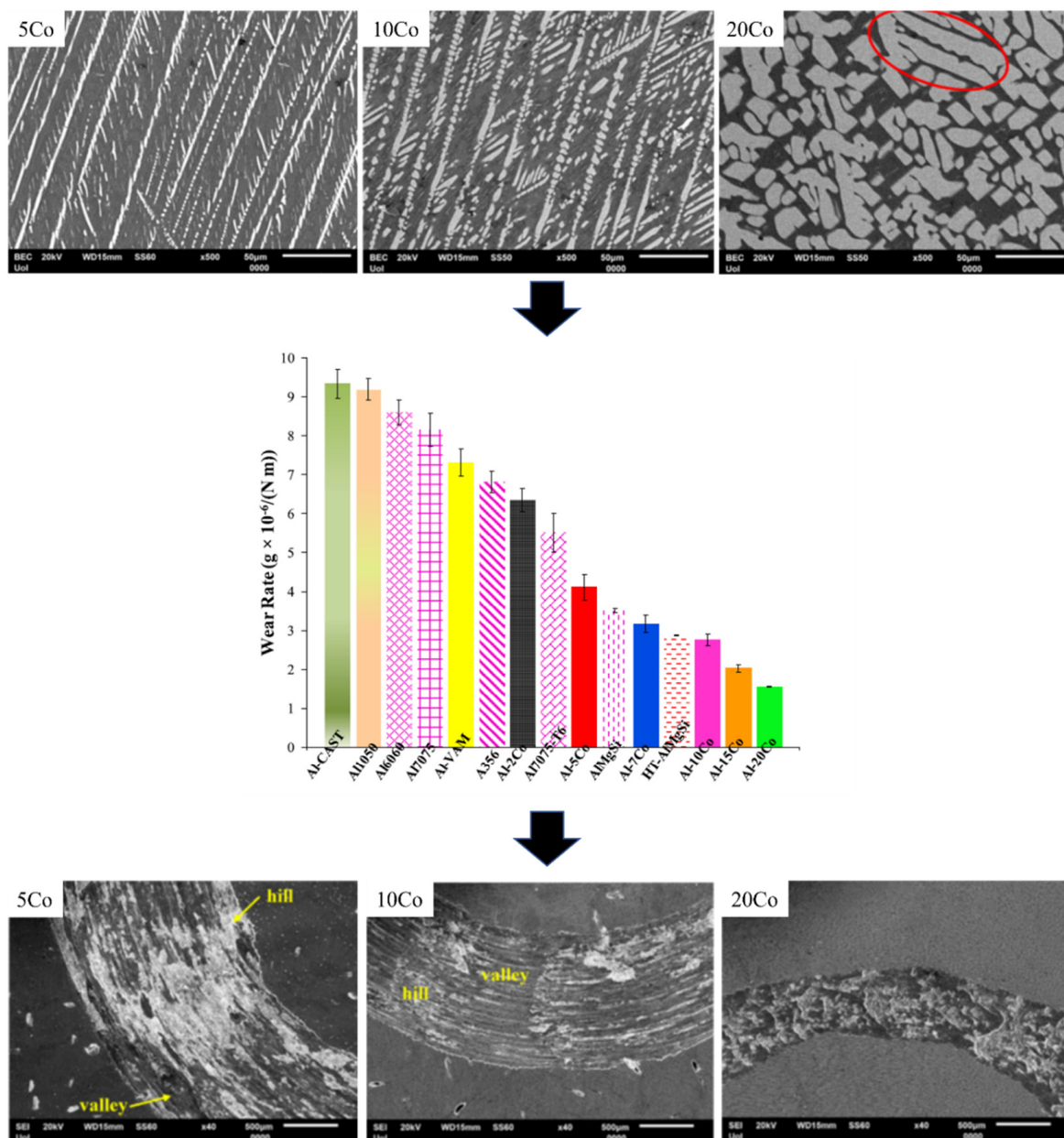


Figure 6. SEM images of Al-5 wt %Co, Al-10 wt %Co and Al-20 wt %Co (Red eclipse: side branching) as fabricated by vacuum arc melting and after sliding wear (ball on disk, 1000 m sliding distance, AISI 52100 steel counter body). Wear rates for Al-Co alloys (2–20 wt % Co) under sliding wear compared to various commercial Al alloys (Al1050, Al6060, Al7075, Al7075-T6, A356, AlMgSi) (Reprinted with permission from [35], Copyright 2022, Elsevier).

7. Prospects and Potential Applications

Al-Co alloys is an emerging category of metallic materials of high interest that can be fabricated with the employment of a variety of techniques to optimize their microstructures

and therefore their performance. Al-Co alloys can be fabricated with low cost, versatile techniques such as stir casting, well established techniques used in the industry such as vacuum arc melting and laboratory scale techniques such as melt spinning. Modern fabrication techniques such as additive manufacturing have been successfully used to manufacture Al-Co alloys. Fabrication techniques that employ a fast solidification rate are of high interest due to the microstructural outcomes that evolve with the formation of fine precipitates and supersaturated solid solutions. Regardless of the fabrication method, Al-Co alloys exhibit good corrosion and wear resistance. Non-equilibrium processed Al-Co alloys have favorable surface degradation properties compared to conventionally produced Al-Co alloys due to their refined microstructure. Increasing Co content leads to an increasing volume fraction of intermetallics and the formation of different Co-rich intermetallics. An obvious downside is the decrease in the volume fraction of ductile Al and thus the increasing brittleness of the alloy. Furthermore, increasing Co content leads to increasing density and increasing raw material costs. An interesting observation is that the corrosion behavior of Al-Co alloys does not appear to be very sensitive to the Co content (3.5% NaCl solution and 1M H₂SO₄ solution) as far as the Al-Al₉Co₂ part of the Al-Co system is concerned. On the other hand, when multiple intermetallics are formed (≥ 32 wt % Co), the corrosion behavior is more complex due to the formation of multiple galvanic cells. Intermetallic compounds with increasing Co content appear to be more corrosion resistant. When it comes to wear resistance, the outcome is more ambiguous. While the intermetallic Al₉Co₂ has a beneficial role in strengthening the Al matrix, leading to improved resistance to sliding wear, the increasing volume fraction of intermetallic compounds decreases ductility. While it is known that the precipitation of Al₉Co₂ in Al-Co alloys leads to increased hardness, it is not understood how the fabrication method and the Co content affects the mechanical properties and the deformation mechanisms.

Taking into account the good surface degradation properties of low Co containing Al-Co alloys in comparison with commercial Al alloys, the relatively high cost of Co and the increasing density and brittleness of Al-Co alloys with increasing Co content, it is suggested that Al-Co alloys with modest Co content could be a useful alternative to the widely used Al alloys in aggressive environments. Al-Co alloys of low Co content are of interest in the automotive and aerospace industries, especially in applications that require high sliding wear resistance and good corrosion performance while maintaining relatively low density and reasonable raw material costs. The use of high Co containing Al-Co alloys is limited by the relatively low ductility. Nonetheless, taking into account the good corrosion, wear and oxidation resistance, those compositions can find potential applications as coatings in demanding environments.

8. Conclusions

In this work, the developments of the emerging field of Al-Co alloys have been discussed, including phase constitution, fabrication routes, microstructure, mechanical and surface degradation properties.

Over the years, Al-Co alloys have been successfully fabricated with a variety of different techniques spanning from conventional stir casting to rapid solidification techniques such as melt spinning. Modern techniques such as additive manufacturing have also been successfully employed to fabricate Al-Co alloys. The interest in using these techniques stems mostly from the fact that they enable achieving different cooling rates and therefore achieving different microstructures (refined precipitates, supersaturated solid solutions) with improved properties.

Al-Co alloys exhibit a lot of attractive properties such as good corrosion, wear and oxidation properties, as compared to commercial Al alloys. Low Co-containing Al-Co alloys are potential candidates for applications that require improved surface degradation properties while maintaining reasonable density and production costs. On the other hand, Al-Co alloys of high Co content may find application as coatings in demanding environments due to their good corrosion, wear, and oxidation resistance.

Author Contributions: Conceptualization, A.K.S.; methodology, A.K.S., S.G., A.G.L., S.K. and A.E.K.; validation, A.K.S., S.G. and A.G.L.; formal analysis, A.K.S., S.G. and A.E.K.; investigation, A.K.S. and S.G.; resources, S.K. and S.G.; data curation, A.K.S., S.G. and S.K.; writing—original draft preparation, A.K.S., S.G. and A.G.L.; writing—review and editing, A.K.S. and S.G.; visualization, A.K.S. and S.G.; funding acquisition, S.K. and S.G. All authors have read and agreed to the published version of the manuscript.

Funding: This research was funded by the UK Research & Innovation (UKRI-IUK) national funding agency, grant number 53662 “Design of high-entropy superalloys using a hybrid experimental-based machine learning approach: steel sector application.” The APC was funded by the same grant.

Institutional Review Board Statement: Not applicable.

Informed Consent Statement: Not applicable.

Data Availability Statement: Not applicable.

Conflicts of Interest: The authors declare no conflict of interest.

References

1. Gupta, R.K.; Fabijanic, D.; Dorin, T.; Qiu, Y.; Wang, J.T.; Birbilis, N. Simultaneous improvement in the strength and corrosion resistance of Al via high-entropy ball milling and Cr alloying. *Mater. Des.* **2015**, *84*, 270–276. [[CrossRef](#)]
2. Equivel, J.; Darling, K.A.; Murdoch, H.A.; Gupta, R.K. Corrosion and mechanical properties of Al-5 At. Pct Cr produced by cryomilling and subsequent consolidation at various temperatures. *Metall. Mater. Trans. A* **2018**, *49*, 3058–3065. [[CrossRef](#)]
3. Esquivel, J.; Gupta, R.K. Influence of the V content on the microstructure and hardness of high-energy ball milled nanocrystalline Al-V alloys. *J. Alloy. Compd.* **2018**, *760*, 63–70. [[CrossRef](#)]
4. Witharamage, C.S.; Christudasjustus, J.; Smith, J.; Gao, W.; Gupta, R.K. Corrosion behavior of an in situ consolidated nanocrystalline Al-V alloys. *NPJ Mater. Degrad.* **2022**, *6*, 15. [[CrossRef](#)]
5. Witharamage, C.S.; Christudasjustus, J.; Gupta, R.K. The effect of milling time and speed on solid solubility, grain size, and hardness of Al-V alloys. *J. Mater. Eng. Perform.* **2021**, *30*, 3144–3158. [[CrossRef](#)]
6. Esquivel, J.; Gupta, R.K. Corrosion behavior and hardness of Al-M (M: Mo, Si, Ti, Cr) alloys. *Acta Metall. Sin.* **2017**, *30*, 333–341. [[CrossRef](#)]
7. Kakitani, R.; Reyes, R.V.; Garcia, A.; Spinelli, J.E.; Cheung, N. Relationship between spacing colonies and tensile properties of transient directionally solidified Al-Ni eutectic alloy. *J. Alloy. Compd.* **2018**, *733*, 59–68. [[CrossRef](#)]
8. Esquivel, J.; Wachowiak, M.G.; O’Brien, S.O.; Gupta, R.K. Thermal stability of nanocrystalline Al-5at.% Ni and Al-5at.% V alloys produced by high-energy ball milling. *J. Alloy. Compd.* **2018**, *744*, 651–657. [[CrossRef](#)]
9. Li, M.; Du, S.; Hou, Y.; Geng, H.; Jia, P.; Zhao, D. Study of liquid structure feature of Al_{100-x}Ni_x with resistivity and rapid solidification method. *J. Non-Cryst. Solids* **2015**, *411*, 26–34. [[CrossRef](#)]
10. Carraca, A.P.; Kakitani, R.; Garcia, A.; Cheung, N. Effect of cooling rate on microstructure and microhardness of hypereutectic Al-Ni alloy. *Arch. Civ. Mech. Eng.* **2021**, *21*, 1–9.
11. Esquivel, J.; Murdoch, H.A.; Darling, K.A.; Gupta, R.K. Excellent corrosion resistance and hardness in Al alloys by extended solid solubility and nanocrystalline structure. *Mater Res. Lett.* **2018**, *6*, 79–83. [[CrossRef](#)]
12. Jiang, H.; Liu, Y.C.; Wei, C.; Zhang, Y.H.; Gao, Z.M. Influence of minor Co on the formation of intermetallic phases in the Al₉₁Fe₇Si₂ alloy. *J. Alloy. Compd.* **2008**, *466*, 92–97. [[CrossRef](#)]
13. Wu, X.; Zhang, H.; Zhang, F.; Ma, Z.; Jia, L.; Yang, B.; Tao, T.; Zhang, H. Effect of cooling rate and Co content on the formation of Fe-rich intermetallics in hypereutectic Al₇Si_{0.3}Mg alloy with 0.5% Fe. *Mater. Character.* **2018**, *139*, 116–124. [[CrossRef](#)]
14. Gan, Z.; Wu, H.; Sun, Y.; Su, Y.; Wang, Y.; Wu, C.; Liu, L. Influence of Co content and super gravity-field on refinement of in-situ ultra-fined fibers in Al-2.5Ni eutectic alloys. *J. Alloy. Compd.* **2020**, *822*, 153607. [[CrossRef](#)]
15. Daniels, S. Some sand-cast alloys of aluminium containing cobalt. *Indust. Engin. Chem.* **1926**, *18*, 686–691. [[CrossRef](#)]
16. Garrett, R.K., Jr.; Sanders, T.H., Jr. The formation of coarse intermetallics in rapidly solidified Al-Co alloys. *Mater. Sci. Eng. A* **1983**, *60*, 269–274. [[CrossRef](#)]
17. Menon, J.; Suryanarayana, C. Metallography of a melt quenched Aluminium-Cobalt alloy. *Metallography* **1988**, *21*, 179–197. [[CrossRef](#)]
18. Suryanarayana, C.; Menon, J. Electron microscopy of metastable phases in rapidly solidified Al-Co alloys. *Bull. Mater. Sci.* **1994**, *17*, 121–139. [[CrossRef](#)]
19. Ma, X.L.; Kuo, K.H. Decagonal quasicrystal and related crystalline phases in slowly solidified Al-Co alloys. *Metal. Trans. A* **1992**, *23A*, 1121–1123. [[CrossRef](#)]
20. Schroers, J.; Holland-Moritz, D.; Herlach, D.M.; Grushko, B.K. Urban, Undercooling and solidification behaviour of a metastable decagonal quasicrystalline phase and crystalline phases in Al-Co. *Mater. Sci. Eng.* **1997**, *A226–A228*, 990–994. [[CrossRef](#)]
21. Heggen, M.; Deng, D.; Feuerbacher, M. Plastic deformation properties of the orthorhombic complex metallic alloy phase Al₁₃Co₄. *Intermetallics* **2007**, *15*, 1425–1431. [[CrossRef](#)]

22. Heggen, M.; Houben, L.; Feuerbacher, M. Metadislocations in the structurally complex orthorhombic alloy $\text{Al}_{13}\text{Co}_4$. *Philos. Mag.* **2008**, *88*, 2333–2338. [[CrossRef](#)]
23. Heidelmann, M.; Heggen, M.; Dwyer, C.; Feuerbacher, M. Comprehensive model of metadislocation movement in $\text{Al}_{13}\text{Co}_4$. *Scr. Mater.* **2015**, *98*, 24–27. [[CrossRef](#)]
24. Allarcon Villaseka, S.; Serkovic Loli, L.N.; Ledieu, J.; Fournee, V.; Gille, P.; Dubois, J.M.; Gaudry, E. Oxygen adsorption on the $\text{Al}_9\text{Co}_2(001)$ surface: First principles and STM study. *J. Phys. Condens. Matter* **2013**, *25*, 355003. [[CrossRef](#)] [[PubMed](#)]
25. Allarcon Villaseka, S.; Ledieu, J.; Serkovic Loli, L.N.; de Weerd, M.C.; Gille, P.; Fournee, V.; Dubois, J.M.; Gaudry, E. Structural investigation of the (001) surface of the Al_9Co_2 complex metallic alloys. *J. Phys. Chem. C* **2011**, *115*, 14922–14932. [[CrossRef](#)]
26. Addou, R.; Shukla, A.K.; Allarcon Villaseka, S.; Gaudry, E.; Deniozou, T.; Hegger, M.; Feuerbacher, M.; Widmen, R.; Groning, O.; Fournee, V.; et al. Lead adsorption on the $\text{Al}_{13}\text{Co}_4(100)$ surface: Heterogenous nucleation and pseudomorphic growth. *J. Phys.* **2011**, *13*, 103011. [[CrossRef](#)]
27. Kandaskalov, D.; Fourne, V.; Ledieu, J.; Gaudry, E. Adsorption properties of the o- $\text{Al}_{13}\text{Co}_4(100)$ surface towards molecules involved in semihydrogenation of acetylene. *J. Phys. Chem. C* **2014**, *118*, 23032–23041. [[CrossRef](#)]
28. Kandaskalov, D.; Fourne, V.; Ledieu, J.; Gaudry, E. Catalytic semi-hydrogenation of acetylene on the (100) surface of the o- $\text{Al}_{13}\text{Co}_4$ quasicrystalline approximant: A DFT study. *J. Phys. Chem. C* **2017**, *121*, 18738–18745. [[CrossRef](#)]
29. Anand, K.; Fournee, V.; GPrevot, G.; Ledieu, J.; Gaudry, E. No-wetting behaviour of Al-Co quasicrystalline approximants owing to their unique electronic structures. *Appl. Mater. Inter.* **2020**, *12–13*, 15793–15801. [[CrossRef](#)]
30. Allarcon Villaseka, S.; Dubois, J.M.; Gaudry, E. Lead adsorption on the pseudo-10-fold surface of the $\text{Al}_{13}\text{Co}_4$ complex metallic alloy: A first principle study. *Int. J. Quantum Chem.* **2012**, *113*, 1–7.
31. Bobaru, S.; Gaudry, E.; de Weerd, M.C.; Ledieu, J.; Fournee, V. Competing allotropes of Bi deposited on the alloy $\text{Al}_{13}\text{Co}_4(100)$ surface. *Phys. Rev. B* **2012**, *86*, 214201. [[CrossRef](#)]
32. Petucci, J.; Karimi, J.M.; Huang, Y.T.; Curtarolo, C. Ordering and growth of rare gas films (Xe, Kr, Ar, and Ne) on the pseudo-ten-fold quasicrystalline approximant $\text{Al}_{13}\text{Co}_4(100)$ surface. *J. Phys. Condens. Matter* **2014**, *26*, 095003. [[CrossRef](#)]
33. Fourne, V.; Gaudry, E.; Ledieu, J.; de Weerd, M.C.; Diehl, R.D. Quasi-ordered C_{60} molecular films grown on the pseudo-ten-fold (100) surface of the $\text{Al}_{13}\text{Co}_4$ quasicrystalline approximant. *J. Phys. Condens. Matter* **2016**, *28*, 355001. [[CrossRef](#)] [[PubMed](#)]
34. Lekatou, A.G.; Sfikas, A.K.; Karantzalis, A.E. The influence of the fabrication route of the microstructure and surface degradation properties of Al reinforced by Al_9Co_2 . *Mater. Chem. Phys.* **2017**, *200*, 33–49. [[CrossRef](#)]
35. Lekatou, A.G.; Sfikas, A.K.; Sioulas, D.; Kanterakis, D. Sliding wear performance of Al-Co alloys fabricated by vacuum arc melting and correlation with their microstructure. *Mater. Chem. Phys.* **2022**, *276*, 125411. [[CrossRef](#)]
36. Bakoulis, G.; Lekatou, A.G.; Pouliou, A.; Sfikas, A.K.; Lentzaris, K.; Karantzalis, A.E. Al-(Al_9Co_2 - $\text{Al}_{13}\text{Co}_4$) powder metallurgy processed composite materials: Analysis of microstructure, sliding wear and aqueous corrosion. *Mater. Sci. Eng. Adv. Res.* **2017**, *Special Issue*, 53–60.
37. Geng, K.; Yang, Y.; Li, S.; Misra, R.D.K.; Zhu, Q. Enabling high-performance 3D printing by decorating with high laser absorbing Co phase. *Addit. Manuf.* **2020**, *32*, 101012. [[CrossRef](#)]
38. McAllister, A.K. The Al-Co (Aluminium-Cobalt) system. *Bull. Alloy Phase Diagr.* **1989**, *10*, 646–650. [[CrossRef](#)]
39. Elagin, V.I. Ways of developing high-strength and high-temperature structural aluminium alloys in the 21st century. *Met. Sci. Heat Treat.* **2007**, *49*, 427–434. [[CrossRef](#)]
40. Grushko, B.; Wittenberg, R.; Bickmann, K.; Freiburg, C. The contribution of Al-Co alloys between Al_9Co_2 and Al_5Co_2 . *J. Alloy. Compd.* **1996**, *233*, 279–287. [[CrossRef](#)]
41. Simon, P.; Zelenina, I.; Ramlau, R.; Carillo-Cabrera, W.; Burkhardt, U.; Borrmann, H.; Cardoso Gil, R.; Feuerbacher, M.; Gille, P.; Grin, Y. Structural complexity of the intermetallic o- $\text{Al}_{13}\text{Co}_4$. *J. Alloy. Compd.* **2020**, *820*, 153363. [[CrossRef](#)]
42. Fleischer, F.; Weber, T.; Jung, D.Y.; Steurer, W. o'- $\text{Al}_{13}\text{Co}_4$, a new quasicrystal approximant. *J. Alloy. Compd.* **2010**, *500*, 153–160. [[CrossRef](#)]
43. Priputen, J.; Kusy, M.; Drienovsky, M.; Janickovic, D.; Cicka, R.; Cernickova, I.; Janovec, J. Experimental reinvestigation of Al-Co phase diagram in vicinity of $\text{Al}_{13}\text{Co}_4$ family of phases. *J. Alloy. Compd.* **2015**, *647*, 486–497. [[CrossRef](#)]
44. Shevchenko, M.A.; Berezutskii, V.V.; Ivanov, M.I.; Kudin, V.G.; Sudavtsova, V.S. Thermodynamic properties of alloys of the Al-Co and Al-Co-Sc systems. *Russ. J. Phys. Chem. A* **2014**, *88*, 729–734. [[CrossRef](#)]
45. Stein, F.; He, C.; Dupin, N. Melting behaviour and homogeneity range of B2 CoAl and updated thermodynamic description of the Al-Co system. *Intermetallics* **2013**, *39*, 58–68. [[CrossRef](#)]
46. Okamoto, H. Supplemental literature review of binary phase diagrams: Ag-Yb, Al-Co, Al-I, Co-Cr, Cs-Te, In-Sr, Mg-Tl, Mn-Pd, Mo-O, Mo-Re, Ni-Os, V-Ze. *J. Phase Equilib. Diffus.* **2016**, *37*, 726–737. [[CrossRef](#)]
47. Li, X.; Liu, L.B.; Jiang, Y.; Huang, G.X.; Wang, X.; Jiang, Y.R.; Liang, J.S.; Zhang, L.G. Thermodynamic evaluation of phase equilibria and glass-forming ability of the Al-Co-Gd system. *Calphad* **2016**, *52*, 57–65. [[CrossRef](#)]
48. Šulháněk, P.; Drienovský, M.; Černíčková, I.; Ďuriška, L.; Skaudžius, R.; Gerhátová, Ž.; Palcut, M. Oxidation of Al-Co Alloys at High Temperatures. *Materials* **2020**, *13*, 3152. [[CrossRef](#)]
49. Douglas, A.M.B. The structure of Co_2Al_9 . *Acta Cryst.* **1950**, *3*, 19–24. [[CrossRef](#)]
50. Bostrom, M.; Prots, H.; Prots, Y.; Burkhardt, U.; Grin, Y. The Co_2Al_9 structure revised. *Z. Anorg. Allg. Chem.* **2005**, *631*, 534–541.
51. Li, X.Z.; Ma, X.L.; Kuo, K.H. A structural model of orthorhombic Al_3Co , derived from the monoclinic $\text{Al}_{13}\text{Co}_4$ by high-resolution electron microscopy. *Philos. Mag. Lett.* **1994**, *70*, 221–229. [[CrossRef](#)]

52. Grin, J.; Burkhardt, U.; Elner, M.; Peters, K. Crystal structure of orthorhombic $\text{Co}_4\text{Al}_{13}$. *J. Alloy. Compd.* **1994**, *206*, 243–247. [[CrossRef](#)]
53. Hudd, R.C.; Taylor, W.H. The structure of $\text{Co}_4\text{Al}_{13}$. *Acta Cryst.* **1962**, *15*, 441–442. [[CrossRef](#)]
54. Freiburg, C.; Grushko, B.; Wittenberg, R.; Reichert, W. Once more about monoclinic $\text{Al}_{13}\text{Co}_4$. *Mater. Sci. Forum* **1996**, 228–132, 583–586. [[CrossRef](#)]
55. Ma, X.L.; Li, X.Z.; Kuo, K.H. A family of τ -inflated monoclinic $\text{Al}_{13}\text{Co}_4$ phases. *Acta Cryst.* **1995**, *B-51*, 36–43. [[CrossRef](#)]
56. Li, X.Z.; Hiraga, K. High-resolution electron microscopy of the ε - Al_3Co , a monoclinic approximant of the Al-Co decagonal quasicrystal. *J. Alloy. Compd.* **1998**, *269*, L13–L16. [[CrossRef](#)]
57. Mo, Z.M.; Sui, H.X.; Ma, X.L.; Kuo, K.H. Structural models of τ^2 -inflated monoclinic and orthorhombic Al-Co phases. *Mater. Trans. A Phys. Metall. Mater. Sci.* **1998**, *29*, L13–L16. [[CrossRef](#)]
58. Christensen, J.; Oleynikov, P.; Hovmuller, S.; Zou, X.D. Solving approximant structures using a “strong reflections” approach. *Ferroelectrics* **2004**, *305*, 273–277. [[CrossRef](#)]
59. Zhang, H.; Wang, S.J.; Wang, S.C.; Li, Z.C.; Hovmuller, S.; Zou, X.D. A structural model for τ^2 - $\text{Al}_{13}\text{Co}_4$ deduced by the strong relations approach. *J. Comput. Theor. Nanosci.* **2008**, *5*, 1735–1737. [[CrossRef](#)]
60. Sugiyama, K.; Yasuhara, A.; Hiraga, K. Structure of τ^2 - Al_3Co a monoclinic approximant of the Al-Co decagonal quasicrystals. In *Aperiodic Crystals*; Smidt, S., Withers, R.K., Lifshitz, R., Eds.; Springer: Dordrecht, The Netherlands, 2013; pp. 237–242.
61. Bradley, A.J. Crystal structure of Co_2Al_5 . *Z. Krist.* **1938**, *99*, 480–487.
62. Newkirt, J.B.; Black, P.J.; Damjanovic, A. The refinement of Co_2Al_5 structures. *Acta Cryst.* **1961**, *14*, 532–533. [[CrossRef](#)]
63. Burkhardt, U.; Ellner, M.; Grin, Y.; Baumgartner, M. Powder diffraction refinement of Co_2Al_5 structure. *Powder Diffr.* **1998**, *13*, 159–162. [[CrossRef](#)]
64. Cooper, M.J. The electron distribution in phases CoAl and NiAl . *Philos. Mag.* **1963**, *8*, 811–821. [[CrossRef](#)]
65. Dutchak, Y.I.; Chekh, V.G. High temperature X-ray diffraction study of the lattice dynamics of the compounds Al-Co and Al-Ni. *Russ. J. Phys. Chem.* **1981**, *55*, 1326–1328.
66. Adam, A.M. Dendrite refinement of Al_9Co_2 compound by a continuous increase of the cooling rate during solidification. *UPB Sc. Bull. Ser. B* **2012**, *74*, 289–300.
67. Adam, A.M. Influence of rapid solidification on the microstructure on aluminium rich hypereutectic Al-Co alloys. *UPB Sc. Bull. Ser. B* **2011**, *73*, 217–228.
68. Hung, C.J.; Nayak, S.K.; Sun, Y.; Fennessy, C.; Vedula, V.K.; Tulyani, S.; Lee, S.W.; Alpay, S.P.; Hebert, R.J. Novel Al-X alloys with improved hardness. *Mater. Des.* **2020**, *192*, 108699. [[CrossRef](#)]
69. Silva, C.A.P.; Kakitani, R.; Cante, M.V.; Bryto, C.; Garcia, A.; Spinelli, J.E.; Cheung, N. Microstructure, phase morphology, eutectic coupled zone and hardness of Al-Co alloys. *Mater. Charact.* **2020**, *169*, 110617. [[CrossRef](#)]
70. Sun, Y.; Hung, C.; Hebert, R.J.; Fennessy, C.; Tulyani, S.; Aindow, M. Eutectic microstructures in dilute Al-Ce and Al-Co alloys. *Mater. Charact.* **2019**, *154*, 269–276. [[CrossRef](#)]
71. Osorio, W.R.; Spinelli, J.E.; Ferreira, I.L.; Garcia, A. The roles of macrosegregation and of dendritic array spacings of the electrochemical behavior of an Al-4.5 wt.% Cu alloy. *Electrochim. Acta* **2007**, *52*, 3265–3273. [[CrossRef](#)]
72. Lekatou, A.; Sfikas, A.K.; Karantzalis, A.E.; Sioulas, D. Microstructure and corrosion performance of Al-32%Co alloys. *Corros. Sci.* **2012**, *63*, 193–209. [[CrossRef](#)]
73. Brodova, I.G.; Men’Shikova, S.G.; Lad’yanov, V.I.; Yablonskikh, T.I.; Bel’tyukov, A.L.; Astaf’ev, V.V. Crystallization of eutectic alloys $\text{Al}_{88.8}\text{Co}_{11.2}$ under equilibrium and nonequilibrium conditions. *Met. Sci. Heat Treat.* **2015**, *57*, 344–349. [[CrossRef](#)]
74. Men’Shikova, S.G.; Shirinkina, I.G.; Brodova, I.G.; Lad’yanov, V.I.; Suslov, A.A. Structures of thin ribbons from an Al-Co alloy under rapid cooling. *Met. Sci. Heat Treat.* **2016**, *58*, 393–399. [[CrossRef](#)]
75. Froes, F.H. Rapid solidification of lightweight metals alloys. *Mater. Sci. Eng.* **1989**, *A117*, 19–32. [[CrossRef](#)]
76. Lekatou, A.; Sfikas, A.K.; Petsa, C.; Karantzalis, A.E. Al-Co Alloys Prepared by Vacuum Arc Melting: Correlating Microstructure Evolution and Aqueous Corrosion Behavior with Co Content. *Metals* **2016**, *6*, 46. [[CrossRef](#)]
77. Van Tendeloo, G.; Menon, J.; Suryanarayana, C. An electron microscopic study of rapidly solidified Al-5 wt% Co alloy. *J. Mater. Res.* **1987**, *2*, 547–556. [[CrossRef](#)]
78. Sfikas, A.K.; Lekatou, A.G. Electrochemical behavior of Al- Al_9Co_2 in sulfuric acid. *Corros. Mater. Degrad.* **2020**, *1*, 249–272. [[CrossRef](#)]
79. Palcut, M.; Priputen, P.; Kusy, M.; Janovec, J. Corrosion behaviour of Al-29at%Co in aqueous NaCl. *Corros. Sci.* **2013**, *75*, 461–466. [[CrossRef](#)]
80. Palcut, M.; Priputen, P.; Salgo, K.; Janovec, J. Phase constitution and corrosion resistance of Al-Co alloys. *Mater. Chem. Phys.* **2015**, *166*, 95–104. [[CrossRef](#)]
81. Priputen, P.; Palcut, M.; Babinec, M.; Misik, J.; Cernickova, I.; Janovec, J. Correlation between microstructure and corrosion behaviour of near equilibrium Al-Co alloys in various environments. *J. Mater. Eng. Perform.* **2017**, *26*, 3970–3976. [[CrossRef](#)]
82. Browmik, A.; Dolbnya, I.P.; Britton, T.B.; Jones, N.G.; Sernicola, G.; Walter, C.; Gille, P.; Dye, D.; Clegg, W.J.; Giuliani, F. Using coupled micropillar compression and micro-Laue diffraction to investigate deformation mechanisms in a complex metallic alloy $\text{Al}_{13}\text{Co}_4$. *Appl. Phys. Lett.* **2016**, *108*, 1111902.
83. Korte-Kerzel, S.; Schnabel, V.; Clegg, W.J.; Heggen, M. Room temperature plasticity in m- $\text{Al}_{13}\text{Co}_4$ studied by microcompression and high-resolution scanning transmission electron microscopy. *Scr. Mater.* **2018**, *148*, 327–330. [[CrossRef](#)]

84. Walter, C.; Wheeler, J.M.; Barnard, J.S.; Raghavan, R.; Korte-Kerzel, S.; Gille, P.; Michler, J.; Clegg, W.J. Anomalously yielding in the complex metallic alloy $\text{Al}_{13}\text{Co}_4$. *Acta Mater.* **2013**, *61*, 7189–7196. [[CrossRef](#)]
85. Xue, S.; Li, Q.; Xie, D.Y.; Zhang, Y.F.; Wang, H.; Wang, H.; Wang, J.; Zhang, X. High strength, deformable nanotwinned Al-Co alloys. *Mater. Res. Lett.* **2019**, *7*, 33–39. [[CrossRef](#)]
86. do Nascimento, A.M.; Ielardi, M.C.F.; Kina, A.Y.; Tavares, S.S.M. Pitting corrosion resistance of cast duplex stainless steels in 3.5% NaCl solution. *Mater. Charact.* **2008**, *59*, 1736–1740. [[CrossRef](#)]
87. Lifka, B. Corrosion of aluminum and aluminium alloys. In *Corrosion Engineering Handbook*; Schweitzer, P.A., Ed.; Marcel Dekker: New York, NY, USA, 1996; pp. 99–155.
88. Esquivel, J.; Gupta, R.K. Review—Corrosion resistant metastable Al alloys: An overview of corrosion mechanisms. *J. Electrochem. Soc.* **2020**, *167*, 081504. [[CrossRef](#)]
89. Davis, J.R. *Corrosion of Aluminum and Aluminum Alloys*; ASM International: Materials Park, OH, USA, 1999.
90. Gousia, V.; Tsioukis, A.; Lekatou, A.; Karantzalis, A.E. Al-MoSi₂ composite materials: Analysis of microstructure, sliding wear, solid particle erosion, and aqueous corrosion. *J. Mater. Eng. Perform.* **2016**, *25*, 3107–3120. [[CrossRef](#)]
91. Lekatou, A.; Karantzalis, A.E.; Evangelou, A.; Gousia, V.; Kaptay, G.; Gacsi, Z.; Baumli, P.; Simon, A. Aluminium reinforced by WC and TiC nanoparticles (ex-situ) and aluminide particles (in-situ): Microstructure, wear and corrosion behaviour. *Mater. Des.* **2015**, *65*, 1121–1135. [[CrossRef](#)]
92. Wu, J.M.; Li, Z.Z. Contributions of the particulate reinforcement to dry sliding wear resistance of rapidly solidified Al-Ti alloys. *Wear* **2000**, *244*, 147–153. [[CrossRef](#)]
93. Lentzaris, K.; Lekatou, A.G.; Ntoumazios, A.; Karantzalis, A.E.; Sfikas, A.K. Solid particle erosion of aluminum in-situ reinforced with a cobalt aluminide. *Mater. Sci. Eng. Adv. Res.* **2017**, 19–25. Available online: <http://verizonaonlinepublishing.com/MSCPDF/MaterialScienceandEngineeringwithAdvancedResearch3S.pdf> (accessed on 10 May 2022).